Video-Based Lane Estimation and Tracking for Driver Assistance: Survey, System, and Evaluation

Joel C. McCall and Mohan M. Trivedi

Abstract—**Driver-assistance systems that monitor driver intent, warn drivers of lane departures, or assist in vehicle guidance are all being actively considered. It is therefore important to take a critical look at key aspects of these systems, one of which is lane-position tracking. It is for these driver-assistance objectives that motivate the development of the novel "video-based lane estimation and tracking" (VioLET) system. The system is designed using steerable filters for robust and accurate lane-marking detection. Steerable filters provide an efficient method for detecting circular-reflector markings, solid-line markings, and segmented-line markings under varying lighting and road conditions. They help in providing robustness to complex shadowing, lighting changes from overpasses and tunnels, and road-surface variations. They are efficient for lane-marking extraction because by computing only three separable convolutions, we can extract a wide variety of lane markings. Curvature detection is made more robust by incorporating both visual cues (lane markings and lane texture) and vehicle-state information. The experiment design and evaluation of the VioLET system is shown using multiple quantitative metrics over a wide variety of test conditions on a large test path using a unique instrumented vehicle. A justification for the choice of metrics based on a previous study with human-factors applications as well as extensive ground-truth testing from different times of day, road conditions, weather, and driving scenarios is also presented. In order to design the VioLET system, an up-to-date and comprehensive analysis of the current state of the art in lane-detection research was first performed. In doing so, a comparison of a wide variety of methods, pointing out the similarities and differences between methods as well as when and where various methods are most useful, is presented.**

Index Terms—**Active safety systems, intelligent vehicles, lane detection, lane-departure warning, machine vision, performance metrics.**

I. Introduction

WITHIN the last few years, research into intelligent vehicles has expanded into applications that work with or for the human user. Human-factors research is merging with intelligent-vehicle technology to create a new generation of driver-assistance systems that go beyond automated control systems by attempting to work in harmony with a human operator. Lane-position determination is an important component of these new applications. Systems that monitor the driver's state [1], predict driver intent [2], [3], warn drivers of lane departures [4], and/or assist in vehicle guidance [5], [6] are all emerging [7]. With such a wide variety of system objectives, it is important that we examine how lane position is detected and measure performance with relevant metrics in a variety of environmental conditions.

There are three major objectives of this paper. The first is to present a framework for comparative discussion and development of lane-detection and position-estimation algorithms. The second is to present the novel "video-based lane estimation and tracking" (VioLET) system designed for driver assistance. The third is to present a detailed evaluation of the VioLET system by performing an extensive set of experiments using an instrumented-vehicle test bed. To this end, the paper is arranged in the following manner. In Section II, we will first explore the system objectives, environmental variations, and sensing modalities involved in creating a lane-position tracker. In Section III, we will introduce a common framework for lane-position-tracking systems, which we will use to provide comparisons between existing systems based on the objectives, conditions, and sensing systems described in the introduction. Next, in Section IV, we will present the VioLET system, a lane-position detection and tracking system with its design based upon a driver-assistance system for use in a highway road environment. Finally, in Section V, we will evaluate the VioLET system with both: a) a wide variety of performance metrics that are relevant to the system objectives; and b) a wide range of environmental variations and driving contexts.

The contributions of this research extend to five areas.

1) The introduction of a fully integrated lane-estimation-and-tracking system with specific applicability to driver-assistance objectives. By working closely with human-factors groups to determine their needs for lane detection and tracking, we developed a lane-tracking system for objectives such as driver-intent inferencing [8] and behavioral analysis [9].
2) The introduction of steerable filters for robust and accurate lane-marking extraction. As will be described in Section IV, steerable filters provide an efficient method for detecting circular-reflector markings, solid-line markings, and segmented-line markings under varying lighting and road conditions. They help to provide robustness to complex shadowing, lighting changes from overpasses and tunnels, and road-surface variations. Steerable filters are efficient for lane-marking extraction because by computing only three separable convolutions, we can extract a wide variety of lane markings.
3) The incorporation of visual cues (lane markings and lane texture) and vehicle-state information to help

Manuscript received December 28, 2004; revised April 27, 2005, July 26, 2005, and September 14, 2005. The Associate Editor for this paper was N. Papanikolopoulos.

The authors are with the Computer Vision and Robotics Research Laboratory, University of California, San Diego, CA 92093 USA (e-mail: jmccall@ucsd.edu; mtrivedi@ucsd.edu).

Digital Object Identifier 10.1109/TITS.2006.869595

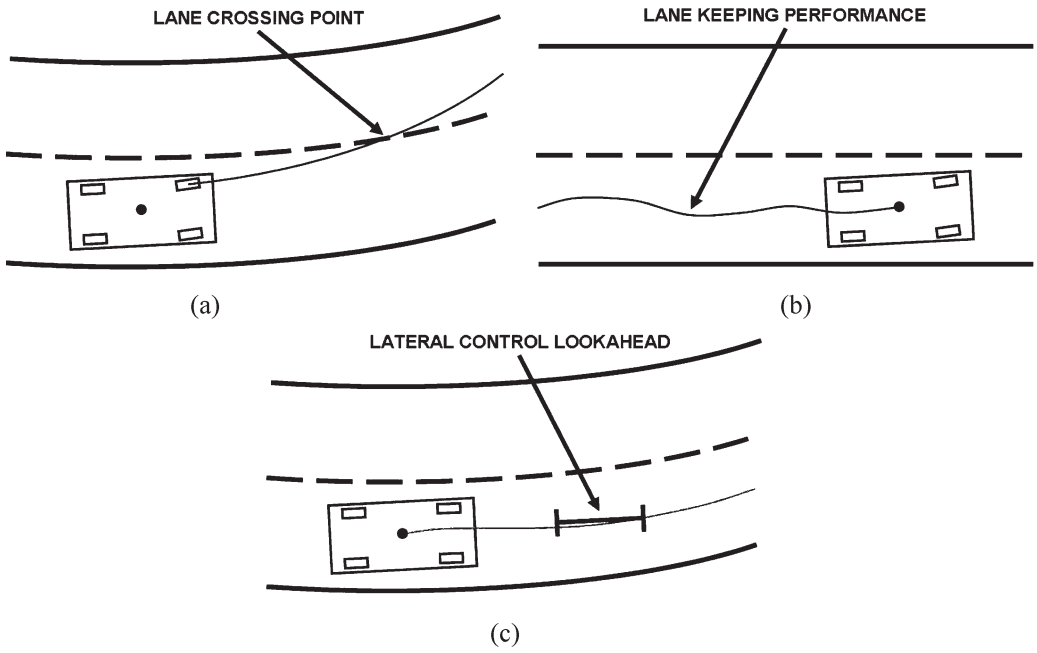

Fig. 1. Illustrations of systems that require lane position, and key performance metrics associated with the system objectives. (a) Lane-departure warning, (b) driver-attention monitoring, and (c) vehicle control.

generate robust estimates of lane curvature, as described in Section IV-C. By using the vehicle-state information to detect an instantaneous road curvature, we can detect a curvature in situations where roadway lookahead is limited.

4) The experiment design and evaluation of the VioLET system. This experimentation was performed using multiple quantitative metrics over a wide variety of test conditions on a large test path using a unique instrumented vehicle. We also present a justification for our choice of metrics based on our work with human-factors applications as well as extensive ground-truth testing from different times of day, road conditions, weather, and driving scenarios.
5) The presentation of an up to date and comprehensive analysis of the current state of the art in lane-detection research. We present a comparison of a wide variety of methods, pointing out the similarities and differences between methods as well as for what objectives and environmental conditions various methods are most useful.

II. Lane-Position Detection: Objectives, Environments, and Sensors

A. System Objectives

In this paper, we will look at three main objectives of lane-position-detection algorithms, as illustrated in Fig. 1. These three objectives and their distinguishing characteristics are the following.

1) *Lane-Departure-Warning Systems*: For a lane-departure-warning system, it is important to accurately predict the trajectory of the vehicle with respect to the lane boundary [10], [11].
2) *Driver-Attention Monitoring Systems*: For a driver-attention monitoring system, it is important to monitor the driver's attentiveness to the lane-keeping task. Measures such as the smoothness of the lane following are important for such monitoring tasks [1].
3) *Automated Vehicle-Control Systems*: For a vehicle-control system, it might be required that the lateral-position error at a specific lookahead distance, as shown in Fig. 1(c), be bounded so that the vehicle is not in danger of colliding with any object [12].

For each objective, it is important to examine the role that the lane-position sensors and algorithms will take in the system and design the system accordingly. Also, the evaluation of these sensors and algorithms must be performed using the proper metrics. Components of lane-position sensors and algorithms that work well for certain objectives and situations might not necessarily work well in others. Examples of these situations will be shown in Section III.

B. Environmental Variability

In addition to the system objective in which the lane-position detection will be used, it is important to evaluate the type of environmental variations that are expected to be encountered. Road markings and characteristics can vary greatly not only between regions, but also over nearby stretches of road. Roads can be marked by well-defined solid lines, segmented lines, circular reflectors, physical barriers, or even nothing at all. The road surface can be comprised of light pavement, dark pavement, or even combinations of different pavements. An example of the variety of road environments can be seen in Fig. 2. All of the images in the figure were taken from roads within a few miles of each other to show the environmental variability even within small regions. Fig. 2(a) shows a relatively simple

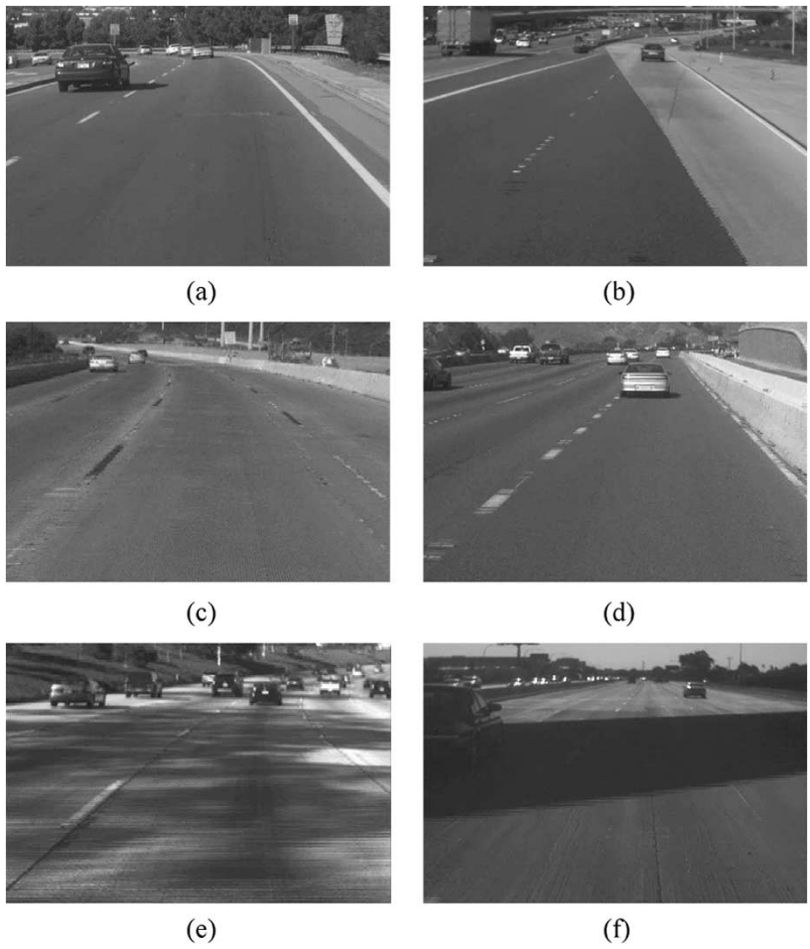

Fig. 2. Images depicting the variety of road markings and conditions for lane-position detection and tracking. (a) Simple road with solid- and segmented-line lane markings; (b) circular reflectors and solid-line lane markings with nonuniform pavement texture; (c) dark on light lane markings with circular reflectors; (d) combination of segmented lines, circular reflectors, and physical barrier marking lane location; (e) highly cluttered shadows from trees obscuring lane markings; and (f) freeway overpass causing extreme lighting changes and reducing road-marking contrast.

Fig. 3. Images of the same stretch of road shown in the daytime and nighttime.

scene with both solid- and segmented-line lane markings. Lane-position detection in this scene can be considered relatively easy because of the clearly defined markings and uniform road texture. Fig. 2(b) shows a more complex scene in which the road surface varies and markings consist of circular reflectors as well as solid lines. Fig. 2(c) shows a road marked solely with circular reflectors. Fig. 2(d) shows a combination of circular and segmented-line markings as well as a physical barrier. Fig. 2(e) and (f) shows complex shadowing obscuring road markings. Along with the various types of markings and road, weather conditions and time of day can have a great impact on the visibility of the road surface, as seen in Figs. 2(e) and (f) and 3.

C. Sensing Modalities

Various sensors have been studied to perform lane-position determination. Examples of these include:

1) camera and vision sensors;
2) internal vehicle-state sensors;
3) line sensors;

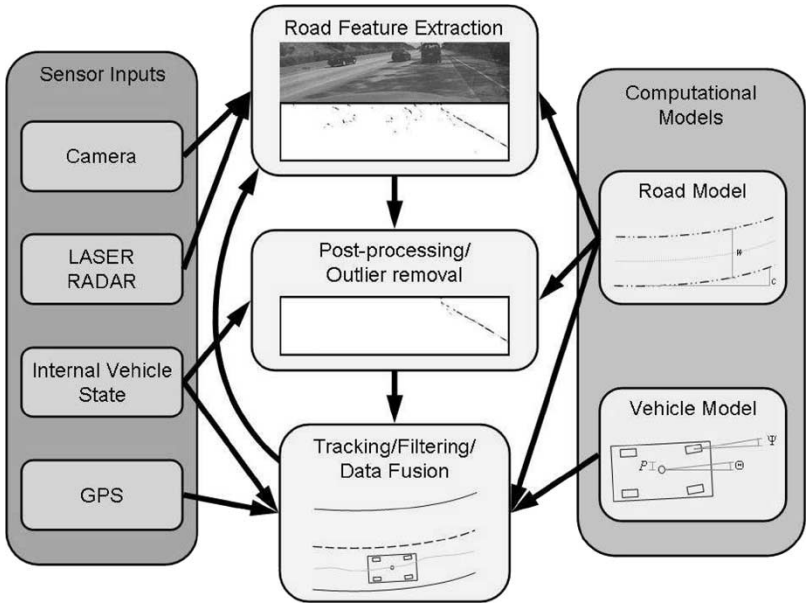

Fig. 4. Generalized flowchart for lane-position-detection systems combining multiple modalities, an iterative detection/tracking loop, and road and vehicle models.

4) LASER radio detection and ranging (RADAR) sensors;
5) global positioning system (GPS) sensors.

While LASER RADAR, line, and GPS sensors can perform extremely well in certain situations, vision sensors can be utilized to perform well in a wide variety of situations. LASER RADAR sensors are useful in rural areas for helping to resolve road boundaries [13], but fail on multilane roads without the aid of vision data. Line sensors, while accurate for current lateral position, have no lookahead and cannot be used well for trajectory forecasting, which is needed to compute metrics such as time to lane crossing (TLC) [10]. GPS, especially differential GPS (dGPS), can provide accurate position resolution, but this requires infrastructure improvements to achieve these accuracies, and to rely on map data that may be outdated and inaccurate. Vision sensors can provide accurate position information without the need for external infrastructure or relying on previously collected map data. In the situations where vision sensors do not perform well (i.e., extreme weather conditions or off-road conditions), the vision data can be fused with other sensor modalities to provide better estimates. This makes vision sensors a good base on which to build a robust lane-position sensing system. Because of these reasons, this paper will focus mainly on vision sensors augmented by vehicle-state information obtained from the in-vehicle sensors.

III. Survey of Lane-Position Detection and Tracking Systems

In this section, we will take a look at the current state of the art in lane-position detection and tracking as well as provide a critical comparison between algorithms. Broad surveys of intelligent vehicles have examined many of the lane-position sensing algorithms available [14], [15]. While these papers are useful for broad examinations of vision research for intelligent vehicles, they are limited in the detail they can provide on lane-position sensing because of their broad nature. It is our intent to provide a more in-depth survey of the current methods for lane-position sensing. In order to cover such a large expanse of research that has taken place in the last 15 to 20 years, we will group the algorithms discussed here into categories related to the contributions of the algorithms.

After taking an extensive look at the types of lane-position-tracking algorithms that have been developed, we have noticed similarities in the way that they are structured. Namely, almost all lane-position-tracking algorithms follow a similar flow. This common system flow is diagramed in Fig. 4. First, a model for the road and vehicle is proposed. This can be something as simple as straight lines or more complex clothoid [16] or spline models [17]. Next, a sensing system is used to gather information about the vehicle's environment. Others have used GPS and other sensors to augment lane-position estimates [18] and fuse the sensor modalities to work in difficult-to-interpret situations like city driving [5]. However, in this article, we will focus on vision sensors combined with vehicle data for reasons described in Section II-C. Features are then extracted from the sensing system. A few examples of these features are edges, motion vectors, and textures. These features are then used in combination with the road model to create an estimate of the lane position. Finally, a vehicle model can then be used to refine these estimates over time given the vehicle data and vision-sensing data. This general flow can vary slightly between systems as objectives of these systems change. For example, Taylor *et al.* [12] propose various control strategies that are tightly coupled with the lane-position tracking. Certain exceptions to this flow also exist. Most notable is the autonomous land vehicle in a neural network (ALVINN) system [19] in which the neural network directly incorporates the feature detection into the control algorithm with no tracking feedback.

A. Road Modeling

Road modeling can greatly increase system performance by helping to eliminate false positives via outlier removal. A variety of different road-modeling techniques have been used. This variety of techniques stems from the wide variety of roads. Bertozzi and Broggi [20] assumed that the road markings form parallel lines in an inverse-perspective-warped image. Others have used approximations to flat roads with piecewise constant curvatures [16], [21]. More recently, deformable contours such as splines have been used to parameterize roads [17], [22]. Maps constructed using dGPS systems have also been used to provide detailed road models in urban environments [5].

The best choice of road model depends on the type of system and intended environment in which the lane-position tracker will be used. For example, complex road models such as spline-based road models might not be a suitable choice for a lane-position control system designed to work on highways, which have a relatively simple structure. Furthermore, a stable control system might only require about a 10-m lookahead [12], making a simple linear road model satisfactory. In a lane-departure-warning system, it is required to calculate the trajectory of the vehicle a few seconds ahead. At freeway speeds, this can require accurate road modeling for 30–40 m or more ahead of the vehicle to catch a TLC of around 1 s. In this situation, a parabolic or spline-based road model would be better. This is because an accurate curvature model is necessary for vehicle-trajectory forecasting.

B. Road-Marking Extraction

Road-marking extraction is a key component to lane-position detection. Road and lane markings can vary greatly, making the generation of a single feature-extraction technique difficult. Edge-based techniques can work well with solid and segmented lines, and can even be extended to attempt to compensate for circular reflectors [23]. However, edge-based techniques can often fail in situations such as those in Fig. 2(b), (e), and (f), which contain many extraneous lines. Frequency-based techniques, such as the Lane-finding in ANother domAin (LANA) system [24], have been shown to be effective in dealing with extraneous edges, but may still be confused by complex shadowing, as seen in Fig. 2(e). The LANA system, in particular, is restricted to diagonal edges, limiting its effectiveness during lane-change maneuvers when the camera is directly above the lane. Other techniques, such as the rapidly adapting lateral position handler (RALPH) system [25], base the lane position on an adaptive road template. These methods generally assume a constant road-surface texture, and therefore can fail in situations such as in Fig. 2(b).

Similar to road modeling, a good choice of a road-marking detection also depends greatly on the type of system and environment in which the lane-position detection is to be performed. If the system is to be used only on certain types of roads only in specific regions, it might not be necessary to detect all possible variations of road markings. For certain system scenarios, such as autonomous vehicle control, it might not be necessary to find specific road markings at all as long as a safe path or lead vehicle to follow [25] can be found.

C. Postprocessing

Postprocessing is necessary to improve estimates based on *a priori* knowledge of the road and extracted features. One of the most common postprocessing techniques used is the Hough transform [26], [27], but other techniques used include enhancing or attenuating features based on orientation [23] or likelihood [21], [24] and culling features based on elevation using stereo vision [22]. Dynamic programming has also been used on extracted line segments to help remove outliers more effectively than Hough transforms [28]. Apostoloff and Zelinsky [29] performed cue scheduling to help determine which of the multiple features should be extracted, processed, and fed into the position-tracking module.

In general, postprocessing is one of the most important steps as it ties together the feature-extraction stage with the tracking stage by generating a robust estimate of actual lane position based on the extracted features. Most postprocessing techniques make assumptions about the road and the vehicle. We will examine these assumptions later in Section III-E

D. Vehicle Modeling and Position Tracking

The two most common tracking techniques used in lane-position-detection systems are Kalman filtering [12], [16] and particle filtering [29], [30]. More complex nonlinear systems have also been used with success [31]. In these systems, feature extraction and position tracking are often combined into a closed-loop feedback system in which the tracked lane position defines an *a priori* estimate of the location and orientation of the extracted features.

Similar with road models, the choice of vehicle models can vary depending on the primary system objective. For objectives such as vehicle control, complex vehicle models might help to improve stability and perform precise movements. Lane-departure-warning systems are often designed for high-speed low-curvature highways. In these situations, a linear approximation to the vehicle model does not significantly affect performance.

E. Common Assumptions and Comparative Analysis

A significant improvement to the accuracy of lane-position estimation can be made by applying a few assumptions based on the structured nature of road surfaces. These assumptions include the following.

1) The road/lane texture is consistent.
2) The road/lane width is locally constant.
3) Road markings follow strict rules for appearance or placement.
4) The road is a flat plane or follows a strict model for elevation change.

Existing algorithms tend to use at least one or more of these assumptions. These assumptions improve overall results; however, it is important to understand where these assumptions might fail, as the lane-position tracking is likely to be used for one of the objectives explored in Section II-A. Any sort of critical failure in these systems could prove disastrous.

The assumption of constant road texture can greatly improve results as the entire road surface is usable as a feature rather than just road markings. In situations in which road markings are scarce or missing, road texture can provide an estimate for lane position [25]. As stated above, roads that have been modified to add lanes or exits [as in Fig. 2(b)] can cause erroneous position estimates.

The assumption that the road or lane width is locally constant can greatly enhance performance by allowing the fusion of left- and right-hand-side boundaries. Three-dimensional (3-D) reconstruction can be performed based on a known constant road width [32]. This assumption is usually valid for most stretches of highway road. However, this is generally not a good assumption for city driving or highways near merging lanes or off ramps. Unfortunately, merging lanes are often critical situations in which you would like to have a robust lane-position estimate.

Road markings are often assumed to be light solid lines on a dark road surface. However, this is not always the case, as can be seen in Fig. 2(d), which contains dark lines on a light road surface as well as circular reflectors. Making assumptions about lane-marking appearance can greatly degrade performance in places where those assumptions about the road infrastructure are not valid.

Often, it is assumed that the road surface is a flat plane or follows a constant-curvature elevation model. This is accurate most of the time and allows monocular vision systems to easily transform points on the image plane to 3-D points in world coordinates. However, for situations such as changing elevations on curves, these road-model assumptions can lead to an incorrect estimation of road curvature. It is important to examine the amount of error in curvature the system can handle before choosing a road model.

Up to this point, we have examined the various modules that make up a lane-position-tracking system, previous research related to each of these modules, and the importance of the modules and the assumptions made about them to the primary objective of the system. It is also important to take a look at systems as a whole and how they compare in performance based on their objectives, environments, and sensing systems. Table I serves to help summarize and compare various lane-position detection and tracking algorithms in relation to the objectives of the system in which they are deployed.

The objectives of many systems, especially the earlier developed systems, were geared towards autonomous vehicle control. The VaMoRs system [16] uses multiple processors and both wide-angle and telephoto lenses for vehicle guidance. A linear vehicle model and 3-D road model were used. The system was tested on a rural road with hills. For autonomous control, the systems can adjust vehicle speed, allowing more time for computation; this is a valid assumption unique to the autonomous control objective. The yet another road follower (YARF) system [33] uses multiple features and robust estimation to help improve performance of the autonomous driving task. Differences in the detected versus expected features are used to identify situations in which the road structure is changing. Taylor *et al.* [12] show a vehicle-control system that they analyzed using a variety of control schemes. Using these different control schemes, they tested their system on an oval test track and measured performance based on the vehicles offset from the centerline. The Driver Assistance using Realtime Vision for INnercity areas (DARVIN) system [5] fuses dGPS information with vision information for supervised autonomous driving in an urban environment. The use of a higher accuracy GPS system provides the benefit of having more exact knowledge of the road structure. dGPS also provides a good *a priori* knowledge about the vehicle's location, which can be improved upon using vision algorithms. However, the use of dGPS makes the system more reliant on a constantly updating infrastructure system and only provides up-to-the-minute knowledge on the vehicle's position. Changes in the road structure, such as construction zones, would need to be relayed to the vehicle for the road model to retain its accuracy. The generic obstacle and lane detection (GOLD) system [20] combined lane-position tracking with obstacle detection for autonomous freeway driving. A special function finds lane markings in an inverse-perspective road image based on brightness differences between a pixel and its neighbors to the left and right. A 3000-km test run was performed and images were shown demonstrating robustness to occlusions and shadows. More recently, the Springrobot [26] used an adaptive randomized Hough transform for processing detected edges.

While the systems mentioned above have focused mainly on the autonomous control objective, others have focused on the lane-departure-warning and driver-assistance objectives. Kwon and Lee [4] developed a system for lane-departure warning based on a modular architecture that allowed fusion of multiple features. The lane position and rate of departure was then fed into a heuristic departure-warning function. Testing was performed based on the overall system performance and quantified in a number of metrics including the detection rate, false-alarm rate, missed-detection rate, and alarm triggering time. The likelihood of image shape (LOIS) system [34] was also used in a lane-departure-warning system. In this system, edge magnitude and orientation was used along with a maximum *a posteriori* estimator to provide lane position. They showed results from a test run with a standard deviation of error of around 13 cm. Risack *et al.* [35] demonstrate a lane-departure-warning system based on the TLC measure. As with most of the other systems, performance was measured for the system as a whole, with little quantitative results related to the lane-position tracking.

Another major difference between the various systems that have been developed stems from the types of environments for which these systems were designed. Ma *et al.* [13] present a system that fuses RADAR information with vision to navigate rural roads. The RADAR images improved performance for weather conditions such as snow, which obstructs the camera view. The DARVIN system mentioned above used GPS to allow navigation through urban areas. The vast majority of systems, however, are designed for highway environments. This is important for the commercial sector, in which a large amount of research has been performed [7].

This analysis and comparison of these systems with respect to their primary objective and intended environment enables us to see some of the merits and deficiencies of these systems. We have seen that improvements to performance can be made

TABLE I
COMPARISON OF VARIOUS LANE-POSITION DETECTION AND TRACKING TECHNIQUES

System	Use[a]	Road Model	Feature Extraction	Postprocessing	Tracking	Evaluation	Comments
VaMoRs (1992) [16]	A	Clothoid Model with vertical curvature	Edge Elements	eliminates points which are not collinear	Linear vehicle dynamics model	Single frame images	Limited processing power. Simple edge detection fails in difficult situations.
YARF (1995) [33]	A	Circular road segments on flat plane	Hue based segmentation and edge detection	Averaging and linear median squares estimation	Operation on single frame	Positive detection rates for feature extraction, single frame images	Multiple detectors. Limited to yellow and white stripes.
ALVINN (1996) [19], [36]	A	Flat road model for generating training data	Image intensity	Neural Network	None	Road tests, various error measure associated with neural networks	Neural network makes it difficult to decouple control from detection, requires lots of training
RALPH (1996) [25]	A B	Constant curvature on flat plane	scan line matched to template	Template matching to slowly evolving near template and fast evolving far template	No inter-frame tracking described	Single frame images	template methods can fail near construction zone or areas where the road has changed. Shows limited quantitative results
GOLD (1998) [20]	C	Constant lane width on flat plane	Adaptive thresholding of pixel differences	Morphological widening	Operation on single frame	Single frame images	Assumes line markings on dark road. some robustness to lighting and occlusion
LOIS (1998) [34]	B A	Parabolic approximation on flat plane	Edge magnitudes and orientations	Maximum a posteriori estimation evaluated by Metropolis algorithm	Kalman filtering	Error histogram from one drive. Standard deviation of error 13cm	Robust to shadowing in presence of strong lane markings. Otherwise untested.
LANA (1999) [24]	B A	Parabolic approximation on flat plane	DCT coefficients for diagonally dominant edges	Maximum a posteriori estimation	Operation on single frame	Single frame images, comparison to LOIS shown	Only using diagonal DCT coefficients limits detection based on orientation of vehicle
Taylor et al. (1999) [12]	A	Constant curvature on flat plane	Template matching	Hough transform	Kalman Filter input into various control schemes	Performance of controllers shown	Focussed on controller performance. Limited real-world testing.
Ma et al. (2000) [13]	A B C	Circular road model on flat plane	Likelihood based on gradient image	Fusion on radar and optical images	Operation on single frame	Single frame images	Designed for elevated or bordered rural roads.
Southall et al. (2001) [30]	C	Curvature and rate of change of curvature	Threshold both pixel values and cross-correlation to dark-bright-dark function	Factored sampling for particle filter	Particle Filtering via CONDENSATION	Estimates shown for an image sequence, no ground truth or quantitative results	Very limited results and testing. Unclear whether feature extraction will work in difficult situations.
Kwon and Lee (2002) [4], [31]	B	Piecewise linear	multiple "feature transformation modules"	combined with data fusion and constraint satisfaction, heuristic departure warning function	nonlinear filtering	analysis of departure warning system given	Good architecture for sensor fusion. Testing limited to false alarm rate of departure warning.
DARVIN (2002) [5]	A B	DGPS based maps of roads	Image gradient	match to DGPS data	nonlinear filtering	selected frames from experimentation	Directed towards urban driving. Heavy reliance on GPS data.
Lee et al. (2003) [37], [38]	B	Straight road on flat plane	Edge distribution function	Hough transform to extract lanes	Not discussed	Detection rate of lane departure warning	Robust to lighting. Will not work for circular reflectors.
Apostoloff et al. (2003) [29]	C	Not discussed	lane markers, road edge, color, width	Cue scheduling to determine which cues are used	Particle Filtering via Distillation	Success rate, mean absolute error for position, yaw, and road width.	Possibly fail in conditions of strong cues that contradict each other (i.e. fig. 2b)
Kang et al. (2003) [28]	D	Straight road on flat plane	Edge direction and magnitude	Connected-component analysis, Dynamic programming	Single frame operation	Qualitative comparison to hough transform based techniques, Single images shown	Focusses on showing visual comparison to hough transform based technique.
Nedevschi et al. (2004) [22]	D	3D model based on clothoids and roll angle	edge detection	outlier removal based on 3D location found with stereo camera system, roll angle detected	Kalman filtering	single images from road scenes with clearly marked lane boundaries	Simple edge detection not robust to shadows, occlusions
This paper (2004)	C B	Parabolic approximation on flat plane	Steerable filters, adaptive road template	Statistical and motion based outlier removal	Kalman Filtering	Extensive error evaluation described in section V-B	

[a] A = Automated Vehicle Control, B = Lane Departure Warning, C = Driver Assistance, D = Unspecified

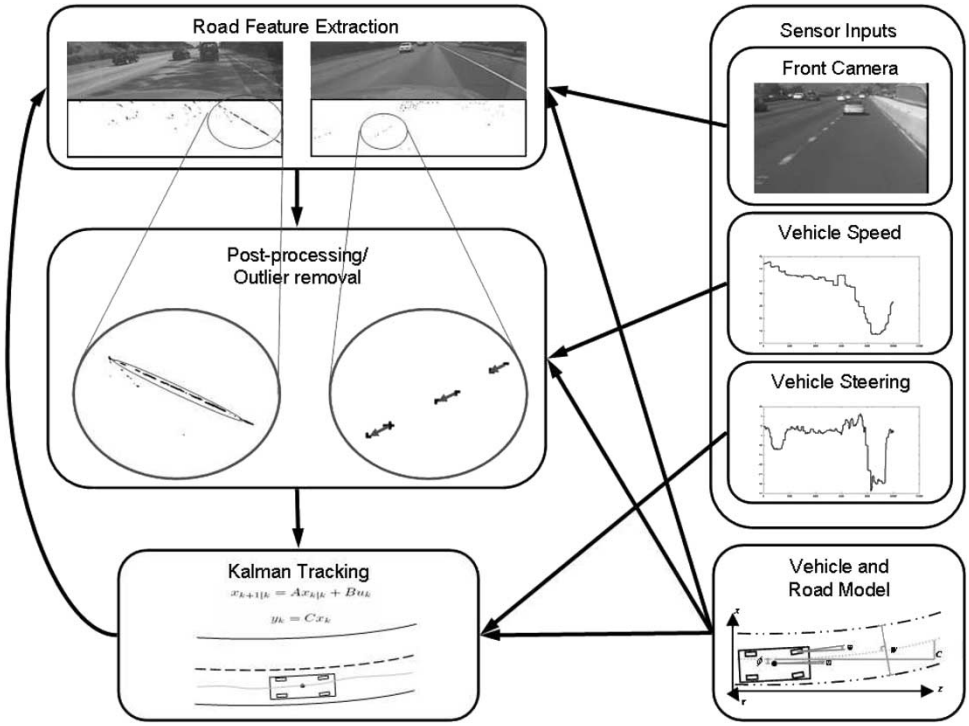

Fig. 5. System flow for VioLET: a driver-assistance focused lane-position estimation and tracking system.

by applying feature extractors that use multiple cues or can be used to extract multiple types of road markings. Assumptions about the road and vehicle models have also been shown to greatly increase performance. However, care needs to be taken that assumptions made about the road environment, which are assumed to apply to a wide range of environments, are not actually limited only to specific regions. Often, testing is performed by the examination of a few key frames or simple tests taken in only a few environments. It was these realizations that led us to develop a lane-tracking system designed for driver-assistance functions capable of performing well under a wider variety of environments. It is also important to provide a thorough evaluation of the system to enable a better comparison of performance between various environments. This includes evaluating the system at different times of the day with varying road markings and textures, as well as taking a close look at special-case scenarios, such as tunnels, to get an accurate quantitative measure of performance.

IV. VioLET System for Driver Assistance

Breaking down the design into the sections illustrated in Fig. 4 helps to create a lane-position detection and tracking system focused on one or more of the system objectives described in Section II-A and capable of handling a variety of the environmental conditions explored in Section II-B. By examining the system one piece at a time and understanding how that choice might affect overall system performance, we can optimize our system for our objective of driver assistance.

The primary objective of the VioLET system is driver assistance. This is a rather broad objective, so some clarification is necessary. It is our intention for the system to provide accurate lateral position over time for the purposes of lane-departure warning and driver-intent inferencing. The intended environment for the lateral-position detection is daytime and nighttime highway driving under a variety of different roadway environments. These environments include shadowing and lighting changes, road-surface-texture changes, and road markings consisting of circular reflectors, segmented lines, and solid lines. The VioLET system follows a similar flow to the generic system flow described in Section III. The system specific flowchart is diagramed in greater detail in Fig. 5. In this section, we will describe each of the system modules and the motivation behind their development.

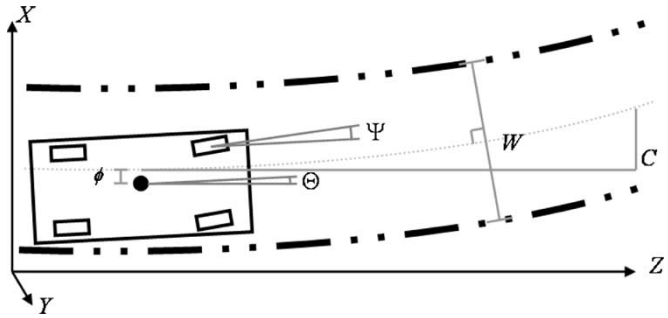

Fig. 6. Vehicle and road models used in the system. We are using a constant-curvature road model and linearized vehicle dynamics for use in a Kalman filter.

A. Vehicle and Road Modeling

Our system objective requires a road and vehicle model that retains accuracy for distances of at least 30–40 m. This is required because in critical situations in which driver-assistance systems are useful, a prediction of the vehicle trajectory at least 1 s ahead of the vehicle is necessary. A simple parabolic road model, as shown in Fig. 6, incorporates position, angle,

and curvature while approximating a clothoid model commonly used in the construction of highway roads [16]. In the figure, $X_{\rm s}$ represents the lateral offset along the center of the road, $Z_{\rm s}$ represents the distance in front of the vehicle, ϕ represents lateral position, θ represents the lane angle, C represents lane curvature, Ψ represents the steering angle, and W represents the lane width. Equation (1) describes the road down the center of the lane, while (2) describes the road at the lane boundaries. l takes the value of 1 for the left lane and -1 for the right lane. Lane width is assumed locally constant, but is updated via a Kalman filter described in Section IV-E. The vehicle dynamics are approximated using a bicycle model similar to that used in [12].

$$X_{\rm s}(Z_{\rm s}) = \phi + \theta Z_{\rm s} + C Z_{\rm s}^2 \tag{1}$$

$$X_{\rm border}(Z_{\rm s}) = \phi + \theta Z_{\rm s} + C Z_{\rm s}^2 + \frac{lW}{2(\theta + C Z_{\rm s})^2 + 2} \tag{2a}$$

$$Z_{\rm border}(Z_{\rm s}) = Z_{\rm s} - \frac{lW(\theta + C Z_{\rm s})}{2(\theta + C Z_{\rm s})^2 + 2}. \tag{2b}$$

B. Road-Feature Extraction

Road-feature extraction is a difficult problem for a variety of reasons. For our objective and intended environment, it is necessary to have a robust estimate of road features given a variety of road-marking types and road environments. Making the problem even more difficult is the necessity for fast algorithms for feature extraction. To this end, we have found that features extracted by using steerable filters provide robust results for multiple types of lane markings and are able to be decomposed into simple convolutions and arithmetic capable of being implemented in a digital signal processor.

1) Formulation of Steerable Filters: Steerable filters have a number of desirable properties that make them excellent for a lane-position-detection application. First, they can be created to be separable in order to speed processing. By separating the filters into X- and Y-components, the convolution of the filter with an image can be split into two convolutions using the X- and Y-components separately. Second, a finite number of rotation angles for a specific steerable filter are needed to form a basis set of all angles of that steerable filter. This allows us to see the response of a filter at a given angle, and therefore, to tune the filter to specific lane angles or look at all angles at once. This property is useful because circular reflectors will have high responses in all directions, while line markings will have high responses in a single direction.

The steerable filters used for the circular reflectors and lane detection are based on second derivatives of two-dimensional Gaussians.

$$G_{xx}(x,y) = \frac{\partial^2}{dx^2} \mathrm{e}^{\frac{-(x^2+y^2)}{\sigma^2}} = -\left(\frac{2x}{\sigma^2} - 1\right) \frac{2}{\sigma^2} \mathrm{e}^{\frac{-(x^2+y^2)}{\sigma^2}} \tag{3}$$

$$G_{xy}(x,y) = \frac{\partial^2}{dxdy} \mathrm{e}^{\frac{-(x^2+y^2)}{\sigma^2}} = \frac{4xy}{\sigma^4} \mathrm{e}^{\frac{-(x^2+y^2)}{\sigma^2}} \tag{4}$$

$$G_{yy}(x,y) = \frac{\partial^2}{dy^2} \mathrm{e}^{\frac{-(x^2+y^2)}{\sigma^2}} = -\left(\frac{2y}{\sigma^2} - 1\right) \frac{2}{\sigma^2} \mathrm{e}^{\frac{-(x^2+y^2)}{\sigma^2}}. \tag{5}$$

It has been shown that the response of any rotation of the G_{xx} filter can be computed using (6) [39].

$$G2^{\theta}(x,y) = G_{xx} \cos^2\theta + G_{yy} \sin^2\theta + G_{xy} \cos\theta \sin\theta. \tag{6}$$

Taking the derivative of (6), setting it equal to 0, and solving for θ, we can find the values that correspond to the minimum and maximum responses. These responses can be computed by the formulas given in (7) and (8).

$$\theta_{\min} = \arctan\left(\frac{G_{xx} - G_{yy} - A}{2G_{xy}}\right) \tag{7}$$

$$\theta_{\max} = \arctan\left(\frac{G_{xx} - G_{yy} + A}{2G_{xy}}\right) \tag{8}$$

where

$$A = \sqrt{G_{xx}^2 - 2G_{xx}G_{yy} + G_{yy}^2 + 4G_{xy}}. \tag{9}$$

2) Application of Steerable Filters to Road-Marking Detection: Using (6)–(8), we can find the values and angles of the minimum and maximum responses, or the response at a given angle. This is useful for detecting circular reflectors because, for small circular objects, the minimum and maximum responses will be very similar. In order to detect circular reflectors, we can therefore threshold the filtered image for minimum responses that are above a certain value as well as within a certain range of the maximum value. For detecting lanes, the response in the direction of the lane should be near the maximum, and the minimum response should be low. Also, applying a threshold to the difference between the response in the direction of the lane marking and the minimum response, we can detect lanes of a specific angle. Fig. 7(a) shows a typical highway scene with lane markings consisting of both circular reflectors and solid lines. Fig. 7(b) shows the image after being filtered and thresholded by the minimum response value. Fig. 7(c) shows the response to lines in the orientation of the current lane parameters. The filter kernel size was chosen to be roughly three times the expected lane-marker width. Filtering on the inverse-perspective-warped image allows a single kernel size to be used over the entire area of interest.

These results show the usefulness of the steerable filter set for relatively normal highway conditions. This filtering technique is also very useful for dealing with shadowed regions of road. Fig. 8 below shows a road section that is shadowed by trees and the filter response for the lane when it is tuned for that lane angle.

C. Road-Curvature Estimation

Some sections of road within our intended environment are marked solely by circular reflectors, as is seen in Fig. 2(f). These circular reflectors are too small to be seen with the

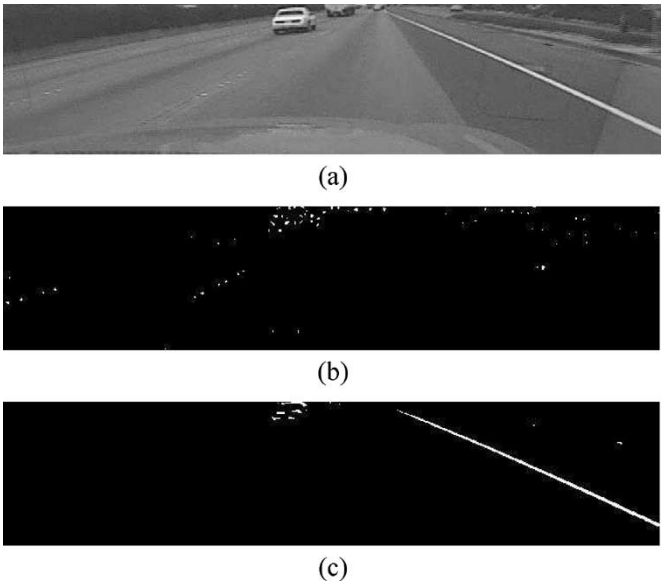

Fig. 7. Application of a steerable filter to road-marking recognition for circular reflectors and solid lines on a highway. (a) Typical highway scene encountered during evaluation. (b) Results of filtering for circular reflectors. (c) Results from the filter for a line tuned to the lane angle.

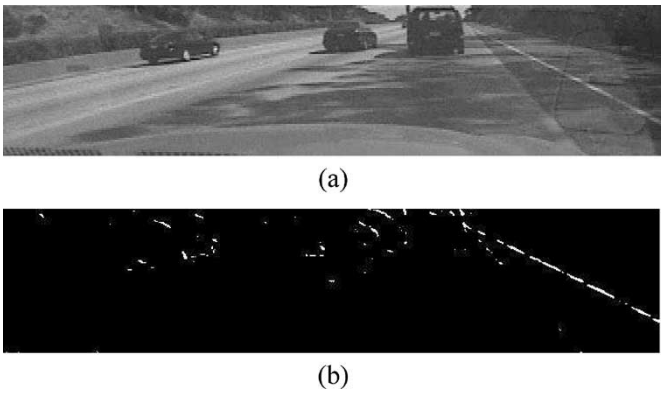

Fig. 8. Filter results when lane markings are shadowed with complex shadows and nonuniform road materials. (a) Highway scene with complex shadowing from trees. (b) Detection results for lines tuned to the lane angle.

cameras used in our configuration at distances greater than about 20 m. In these situations, an adaptive template is used to measure curvature beyond the range of what is detectable by road markings alone. Curvature detection is performed by matching a template of the current road to the road ahead, then fitting the detected results to the lane model described in Section IV-A. The adaptive template is generated per pixel using a weighted average of the intensity values of the previous template and the intensity values of the lane area for the current image. The intensity values for the lane area are found by applying an inverse-perspective warping to the image and cropping a rectangular area centered around the current estimate of the lane position a few meters ahead of the vehicle. The weighting can be adjusted to allow faster or slower response times and is initialized using the intensity values of the initial frame. The template is then matched to the road ahead by minimizing the squared error in intensity values of the inverse-perspective-warped image. The error is minimized laterally

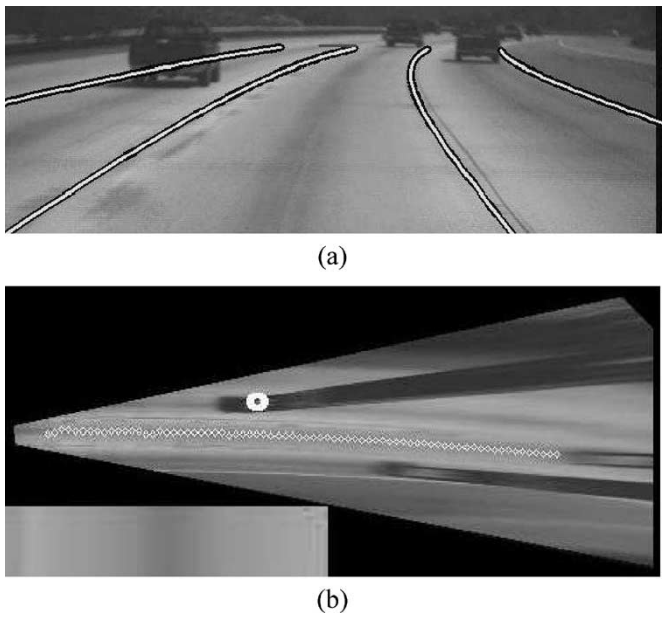

Fig. 9. Curvature detection in the VioLET lane-tracking system. (a) Detected lanes with curvature overlaid onto image. (b) Inverse-perspective warping showing curvature detection (small white dots) and template (lower left corner).

at equally spaced distances ahead of the vehicle to get an estimate of the lateral position of the road at specific distances ahead of the vehicle. The final curvature estimate is generated by minimizing the squared error between the parabolic road model and the measured road positions. While this method works well on most roads with little traffic, template-matching techniques such as these fail in cases of poor road texture and occlusion. For this reason, curvature is also estimated using the vehicles yaw rate and the second derivative of position. These are estimated using the Kalman-filtering equations described in Section IV-E. This provides a robust estimate on lane curvature by combining the vehicle-state information with visual cues from the lane-tracking system to determine instantaneous curvature when road lookahead is not sufficient.

Fig. 9 shows the results of the curvature-detection system. Fig. 9(a) shows a forward-looking view with the detected lane positions overlaid onto the image. Fig. 9(b) shows aerial photography for that specific section of road. The vehicle's trajectory is depicted in this figure using a green curve for future trajectory and a red curve for past trajectory. Fig. 9(c) shows the inverse-perspective warping of the forward-looking camera with the detected lane points shown as small white circles. The template is shown in the lower left-hand corner of Fig. 9(c).

D. Postprocessing and Outlier Removal

In order to perform robust tracking in situations such as in Figs. 2 and 3, postprocessing on the filter results is performed. First, only the filter candidates within the vicinity of the lanes are used in updating the lanes. This removes outliers from other vehicles and extraneous road markings. Because the algorithm uses a local search about the lanes for candidates, it requires initialization. In testing, it was sufficient to initialize the lane-tracker position and trajectory to 0 (corresponding to the center

of the lane). Second, for each lane, the first and second moments of the point candidates are computed. Straight lane markings should be aligned so that there is a high variance in the lane heading direction and a low variance in the other direction. Outliers are then removed based on these statistics. Finally, for circular reflectors, the speed of the vehicle is used to calculate the expected location of the reflector. This is performed using the inverse-perspective equations described in (10). T and R represent the transformation and rotation of the camera, respectively. The world coordinate Y is assumed 0 because of the flat-plane road model. Circular-reflector detections that do not move as predicted by the ground plane are removed as they generally correspond to false detections. These false detections commonly stem from things such as specular highlights on vehicles and other small circular textures that do not move with the ground plane.

$$\begin{bmatrix} x_{\text{image}} \\ y_{\text{image}} \end{bmatrix} = \begin{bmatrix} \frac{X}{Z} \\ \frac{Y}{Z} \end{bmatrix}, \quad \begin{bmatrix} X \\ Y \\ Z \end{bmatrix} = [R \quad T] \begin{bmatrix} X_{\text{world}} \\ 0 \\ Z_{\text{world}} \\ 1 \end{bmatrix}. \quad (10)$$

E. Position Tracking

Position tracking for our objective of driver assistance is vitally important. Position tracking can provide improved results in noisy situations and generate other useful metrics important for the primary system objective. Kalman filtering provides a way to incorporate a linearized version of the system dynamics to generate optimal estimates under the assumption of Gaussian noise. Kalman filtering also provides estimates of state variables that are not directly observable, but may be useful for the system. It is important to have metrics such as rates of change of position robustly estimated not only from lane angles, which may contain errors for vehicle pitch or camera calibration, but also from lane-position estimates over time.

$$x_{k+1|k} = Ax_{k|k} + Bu_k \quad (11)$$

$$y_k = Mx_k \quad (12)$$

where

$$x = [\phi,\ \dot{\phi} = \tan\theta,\ \ddot{\phi},\ W]^{\mathrm{T}} \quad (13)$$

$$A = \begin{bmatrix} 1 & v\Delta t & \frac{(v\Delta t)^2}{2} & 0 \\ 0 & 1 & v\Delta t & 0 \\ 0 & 0 & 1 & 0 \\ 0 & 0 & 0 & 1 \end{bmatrix} \quad (14)$$

$$Bu_k = [0,\ \Phi\Delta t,\ 0,\ 0]^{\mathrm{T}} \quad (15)$$

$$M = \begin{bmatrix} 1 & 0 & 0 & 0 \\ 0 & 1 & 0 & 0 \\ 0 & 0 & 0 & 1 \end{bmatrix}. \quad (16)$$

The Kalman filter state variables are updated using the lane-position and angle estimates along with measurements of steering angle and wheel velocity. These measurements are then used to update the discrete-time Kalman filter for the road and vehicle state. The system and measurement equations as well as the Kalman update equations at time k are detailed in (11)–(16). The variables used in these equations are the same as those described in Section IV-A and Fig. 6. Curvature is currently calculated and filtered separately. Φ is the yaw rate relative to the road. This is calculated separately using the steering angle and road curvature. The initial values for the estimation-error covariance and state-noise covariance were determined by empirical testing. Adding a control input to the Kalman equations allows us to effectively use steering and yaw-rate information from the vehicle similar to that described in [30].

The measurement vector y_k (12) consists of the vehicle position, the lane angle, and the lane width. These measurements are found using a combination of a Hough transform and the lane-marker detection statistics. For solid lane markings, the Hough transform provides a robust means of determining the location and angle of individual lane markings. When a valid line cannot be found using a Hough transform, as in the case of lanes marked with circular reflectors, the statistics of the lane markings are used to determine the position and angle of the lanes. These statistics are described in Section IV-D. This estimation is performed for both the left and right lane markings. These estimates are then used to determine estimates of the lane position, angle, and width using a weighted sum.

V. Experiments and Performance Evaluation

Lane-detection systems have been studied quite extensively and several metrics for the evaluation of lane-position error have been proposed [11], [40]. However, most proposed algorithms have shown limited numerical results or simply selected images of the algorithm results. While these images provide information on the performance on road-marking extraction in specific contexts, they fail to account for errors involved in transforming image coordinates to world coordinates, and cannot be used to quantitatively compare different algorithms. In order to adequately measure the effectiveness of a lane-position detection and tracking system in a specific context or system, specific metrics must be used. In this section, we will explore the usefulness of a variety of performance metrics and show how the algorithm described in this paper performs based on these metrics in a variety of test conditions.

A. System Test-Bed Configuration and Test Conditions

The video input to the system is taken from a forward-looking rectilinear camera for our test results, but can be taken from any number of cameras on our test-bed vehicle. The test bed is shown in Fig. 10. Some of the key capabilities of the Laboratory for Intelligent and Safe Automobiles Infiniti Q45 (LISA-Q) intelligent-vehicle test bed include:

1) eight National Television Standards Committee (NTSC) hardware video compressors for simultaneous capture;
2) controller-area-network (CAN) interface for acquiring steering angle, pedals, yaw rate, and other vehicle information;
3) built-in five-beam forward-looking LASER RADAR range finder;

Fig. 10. LISA-Q intelligent-vehicle test bed. Inset are close-up views of the front camera (left inset) used for detection and tracking and side camera (right inset) used for generating ground truth.

4) wide-area augmentation system (WAAS)-enabled GPS;
5) integration into car audio and after-market video displays for feedback and alerts.

For more information on this test bed, please refer to [41]. Information about the vehicle's state, including wheel velocities and steering angle, are acquired from the car via the internal CAN bus.

Testing was performed on highways in southern California. These highways contained road conditions shown in Figs. 2 and 3, which include

1) lighting changes from overpasses;
2) circular, solid-line, and segmented-line lane markers;
3) shadowing from trees and vehicles;
4) changes in road-surface material.

A camera directed downward at the road on the side of the vehicle provided a good view for generating positional ground-truth data. The cameras used in the system were calibrated for their intrinsic parameters using the Matlab camera calibration toolbox [42].

B. Choice of Metrics for Objective-Specific Performance Evaluation

One of the most common metrics for lane-position performance evaluation is mean absolute error. While this provides a good estimate of the performance of a lane-position tracker for system objectives such as control and driver intent, it lacks usefulness in quantifying the accuracy for other objectives like road-departure warning, in which the TLC and rate of approach to the road boundary are important. For this reason, it is important to use a variety of performance metrics when evaluating a system, rather than just one.

Other statistical metrics that are based on examining the distribution of the detected markings have been proposed [11]. These include the angular-deviation entropy and angular-deviation histogram fraction and their magnitude-weighted counterparts. While these serve as good online metrics for evaluating relative system performance for different stretches of road, they are not as useful for determining system performance relative to a known ground truth.

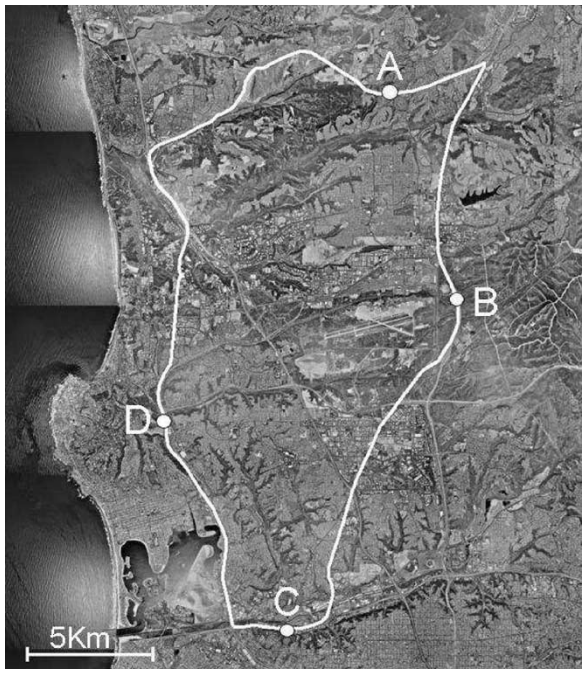

Fig. 11. Route in San Diego (65 km) used in the evaluation. The route is overlayed on aerial photography. Points A, B, C, and D are sections of the road used in the evaluation [photography courtesy of the U.S. Geological Survey (USGS)].

Several metrics have been proposed to evaluate the performance of driver lane-change intent and road-departure-warning systems. These systems are related because they deal with forecasting the vehicle's trajectory. Most of these involve looking at the system as a whole and measuring false positives, false negatives, or the time it takes to trigger an alarm [2], [4], [40]. However, because the systems involve the collection of data other than just the lateral position, it is difficult to decouple the lane-position performance from the system performance using these types of metrics. In order to generate an accurate prediction of performance in a trajectory-forecasting objective, it is necessary to examine the accuracy of the parameters used to generate this forecast. In this situation, we expect the metrics of error distribution of the rate of change of lateral position to provide good indicators of system performance. The rate-of-change-of-the-lateral-position metric was chosen over the time-to-lane-crossing metric for two reasons. First, the rate-of-change metric has been shown to be useful in driver-assistance [38] and driver-intent [8] applications. Second, the time-to-lane-crossing metric is prone to large errors stemming from small errors in vehicle position and lateral velocity. Furthermore, generating a ground truth for the TLC is complicated by the need for a well-known road and vehicle model for the entire stretch of road on which the testing is being performed.

C. Evaluation and Quantitative Results

In order to provide a more complete test of our system, we chose to quantify the error using three different metrics. The three metrics we chose are mean absolute error in position, standard deviation of error in position, and standard deviation of error in rate of change of lateral position.

Fig. 12. Scenes from dawn (row 1), daytime (row 2), dusk (row 3), and nighttime (row 4) data runs for each of the four sections of the road. These scenes show the environmental variability caused by road markings and surfaces, weather, and lighting.

TABLE II
RESULTS FROM THE STANDARD DEVIATION OF THE ERROR PERFORMANCE METRIC EVALUATED UNDER VARIOUS LIGHTING AND ROAD CONDITIONS

	Standard Deviation of Error (cm)				
	Dawn	Noon	Dusk	Night	Total
Set A	4.5400	11.5700	8.1062	7.9710	8.4221
Set B	8.6041	14.8687	7.9457	3.8871	9.6612
Set C	11.1815	13.5135	29.9347	23.2722	20.8885
Set D	5.1547	10.7514	12.1687	8.3031	9.4761
Totals	7.8460	12.7784	17.1246	13.1261	**13.1377**

TABLE III
RESULTS FROM THE MEAN-ABSOLUTE-ERROR PERFORMANCE METRIC EVALUATED UNDER VARIOUS LIGHTING AND ROAD CONDITIONS

	Mean Absolute Error (cm)				
	Dawn	Noon	Dusk	Night	Total
Set A	3.6497	8.6429	5.5313	6.4720	6.0740
Set B	6.8463	10.6362	5.6768	3.0417	6.5503
Set C	8.1815	10.8677	20.4727	12.9471	13.1173
Set D	4.1713	8.4701	9.8390	6.5232	7.2509
Totals	5.7122	9.6542	10.3800	7.2460	**8.2481**

TABLE IV
RESULTS FROM THE DEPARTURE-RATE PERFORMANCE METRIC EVALUATED UNDER VARIOUS LIGHTING AND ROAD CONDITIONS

	Standard deviation of error in departure rate metric (cm/s)				
	Dawn	Noon	Dusk	Night	Total
Set A	0.11107	0.31885	0.18453	0.20120	0.21710
Set B	0.21364	0.32725	0.24030	0.06224	0.23149
Set C	0.26277	0.29709	0.70780	0.39743	0.45173
Set D	0.10842	0.29767	0.19349	0.21076	0.21344
Totals	0.18627	0.31049	0.39693	0.24836	**0.29595**

Results were analyzed according to the metrics discussed in Section V-B under the environmental variations described in Section V-A. More specifically, data were collected from portions of the roughly 65-km route at four different times of the day: dawn, noon, late afternoon/dusk, and night. Scenes from each of these, corresponding to the points A, B, C, and D in Fig. 11, along with an aerial view of the individual points, are shown in Fig. 12. Section A consists of solid-line and segmented-line markers, while sections B and C contained a mixture of segmented lines and circular reflectors. Section D is marked by circular reflectors. Ground truth for 1000 frame sequences was found for each of these locations on the route and each of the four times of the day, making a total of 16 000 testing frames covering many different highway types heading in different directions at different times of the day. These results are shown in Tables II–IV. Per-frame outputs and ground truth for selected data sets can be seen in Figs. 13–15

After examining the results, it is interesting to note that the system actually performs better at night and dawn than during day and dusk. At night, this can be attributed to the larger contrast in road markings due to their reflective nature as well as the lack of complex shadows formed by trees and vehicles during the daytime. Complex shadows hamper the system's ability to detect circular reflectors in scenes such as that shown in Fig. 8. At dawn, a morning fog reduced contrast somewhat, but also helped eliminate shadows. The low contrast of the dawn run require a change in the thresholds used in feature extraction. Future work will include making the system more adaptive to general lighting changes.

Furthermore, the difference in departure-rate performance between daytime and nighttime driving would point to increased number of successful detections (i.e., those not eliminated by outlier removal). The comparatively smaller gain in standard-deviation performance over mean absolute error might suggest that the tracking at night performed better overall, but still contained cases where the tracking was off. This is because the mean-absolute-error metric is less influenced by the small amounts of data points that contain a larger amount of error.

Comparing performance for different types of lane markings, we can see that section A, which contained solid and segmented-line markings, performed better than the other sections, which at points were marked only with circular reflectors.

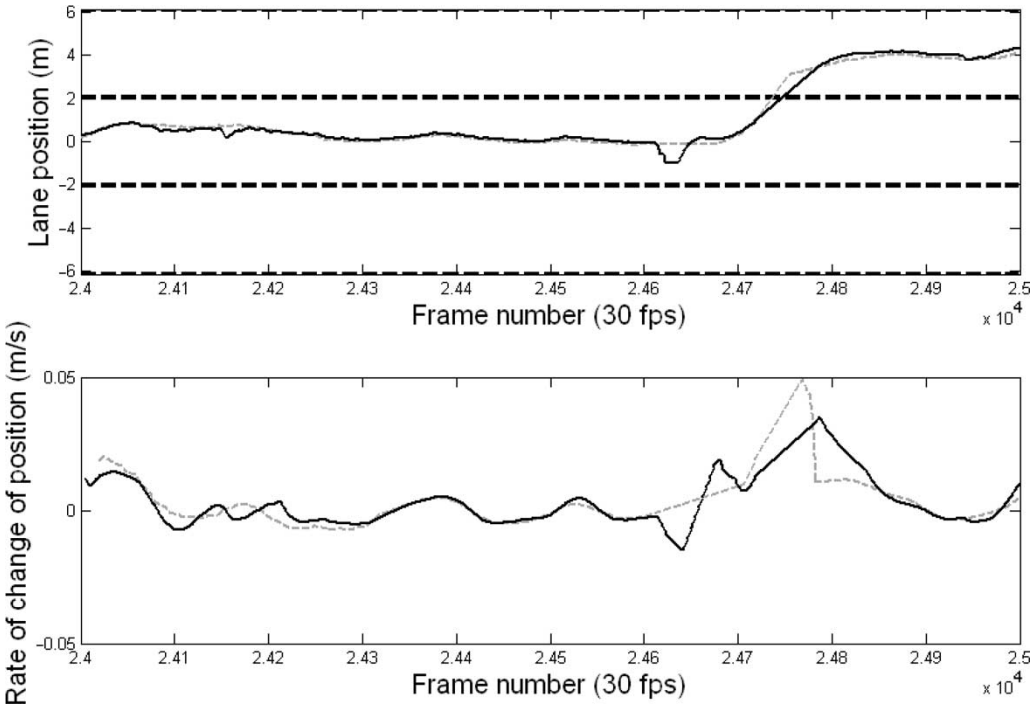

Fig. 13. Lateral position (top) and rate of departure (bottom) for road section A at noon.

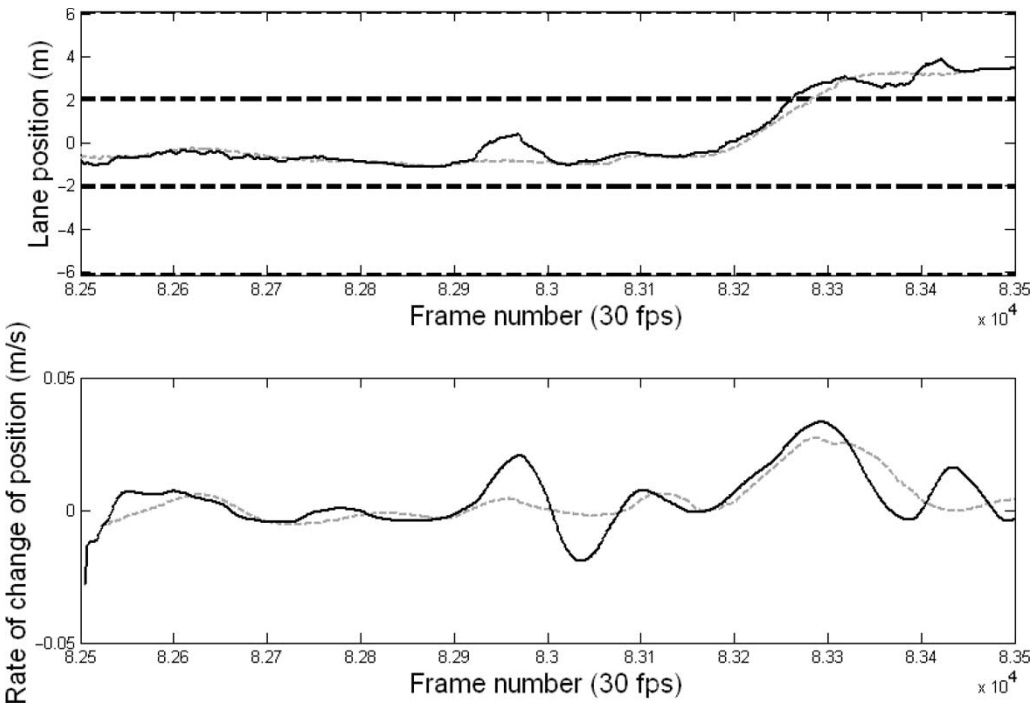

Fig. 14. Lateral position (top) and rate of departure (bottom) for road section C at dusk.

However, this difference is less noticeable than the variations caused by lighting and traffic.

As the system's intended use is in a driver-safety system, it is critical that we analyze the situation in which the lane tracking did not perform well. Section C can be seen to be the most difficult section of road based on the results. Looking deeper into the cause of these errors, we can see points where the tracking is lost for a period of time and then catches back on again. An example of one of these events occurs near frame 82 900 of Fig. 14. Fig. 16 shows this tracking error resulting from occlusion of the road by a vehicle. This section of road is near the intersection of three different freeways, and therefore generally contains more traffic and more people merging and changing lanes. In most of the situations where the tracking was lost, vehicles changed lanes directly in front of the test bed. The specular highlights and lines of the vehicles caused false positives in the feature extraction. Another important event occurred near frame 24 650 of Fig. 13. At this point, the video

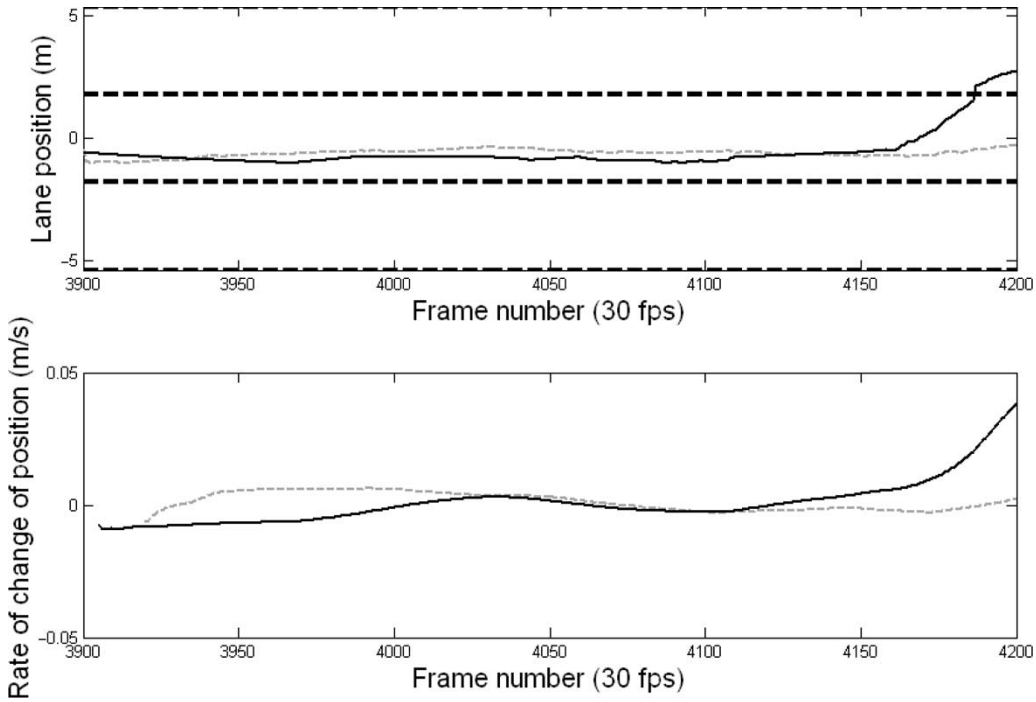

Fig. 15. Lateral position (top) and rate of departure (bottom) for the special-case scenario of traveling through a tunnel. High road curvature at the end of the tunnel results in a loss of tracking.

Fig. 16. Error due to occlusion of the road by a vehicle on the dusk dataset on road segment C.

TABLE V
RESULTS FROM VARIOUS METRICS ASSOCIATED WITH LANE KEEPING VERSUS LANE CHANGING

	Metrics		
	Std. Dev. of Error (cm)	Absolute Mean Error (cm)	Std. Dev. of Error in Rate of Change (cm/s)
Lane Keeping	10.4263	8.2661	0.1625
Lane Changing	16.0634	12.4149	0.4653
Combined	13.0060	9.9446	0.3639

signal was lost due to saturation of the charge-coupled device (CCD) while exiting a tunnel, causing the vertical sync to be misaligned. It is also important to note that while these types of failures might be critical for an autonomous vehicle, a driver-assistance system can warn the driver when the current lane detections do not fit well with previous data and the system is not functioning properly.

D. Lane-Keeping Versus Lane-Changing Performance

Furthermore, the different driving scenarios require different performances for different types of driving. Specifically, lane-departure-warning systems need to accurately detect when the driver is close to the edge of the lane. This makes it important to test the performance during lane changes. Lane-keeping control systems might require good performance only near the center of the lane, where the system is designed to operate. We therefore also measured performance during lane-change maneuvers and compared this with performance during lane keeping.

Table V show the results for the lane-keeping driving context versus the lane-changing driving context. This is an important distinction because some systems, such as lane-departure-warning systems, are required to operate well during lane-changing situations. The data samples used in this evaluation were collected during the day and include circular-reflector markings, dashed-line markings, clear roads, shadowed roads, and overpasses. These data are shown in Figs. 17 and 18. From the table, we can see that there is a performance degradation when changing lanes. This is also evident in the relative higher errors at the peaks and troughs of Fig. 18, which correspond to higher lateral velocities during lane changes. These types of errors are possibly associated with errors in the vehicle model, errors in yaw-rate sensing, and delays associated with Kalman filtering.

E. Special-Case-Scenario Testing

Often, the case is that the situations that can be considered the most critical are less likely to occur. Fig. 19 shows cut scenes from a situation in which the road surface is obfuscated by complex shadows and a tunnel sequence that contains tight quarters and extreme lighting changes. In this section, we will analyze the performance of our lane-position tracker in these two situations.

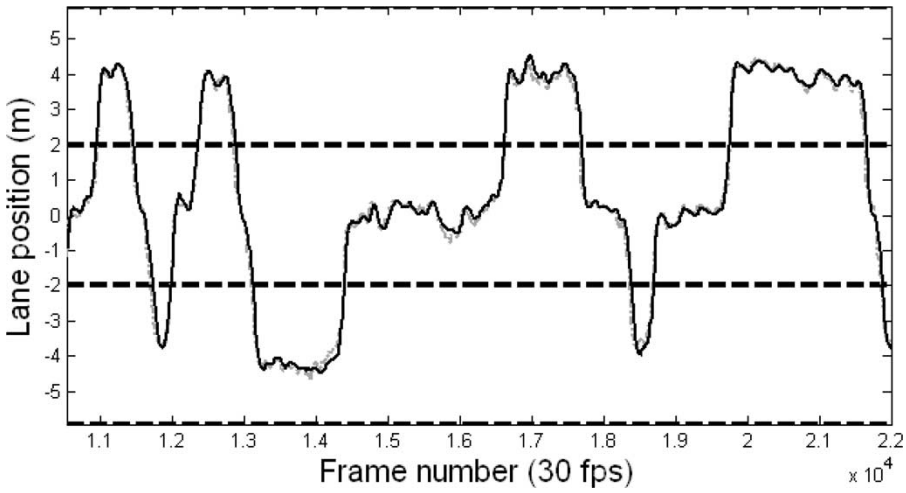

Fig. 17. Detected lateral position (solid black) in meters superimposed on ground truth (dashed gray) plotted versus frame number, with dashed lines marking the position of lane boundaries for an 11 000-frame (slightly over 6 min) sequence.

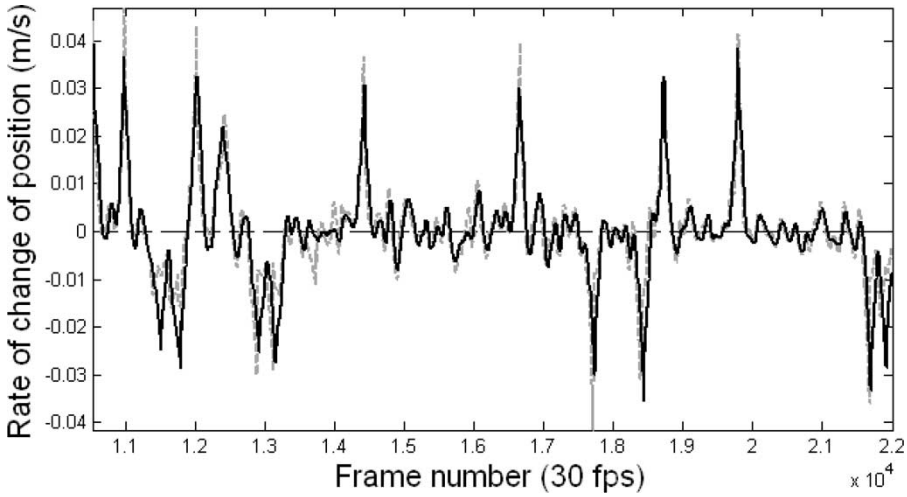

Fig. 18. Detected departure rate (solid black) in meters per second superimposed on ground truth (dashed gray) plotted versus frame number, with dashed line marking the abscissa for the same sequence shown in Fig. 11.

Fig. 19. Scenes from the special-case scenarios of complex shadowing (top row) and tunnels (bottom row). These scenes highlight the extreme variability that can occur within short sections of the road.

First, we will examine the performance while traveling through tunnels. Unfortunately, tunnels are not common in the area where testing was performed so only one tunnel in a more urban setting was used in the testing. The results from the evaluation are quantified in Table VI. At the end of the tunnel was a sharp left-hand turn for which tracking failed as our road model was not designed for such use. Fig. 15 shows the detected position superimposed on ground truth.

The second special case was traveling through complex shadows. Often, trees, overpasses, cars, and other objects can cast shadows with sharp edges and complex shapes. These can pose problems for lane-tracking systems because they form extraneous edges, obscure the road texture, and otherwise complicate feature detection. The results from the evaluation can be seen in Table VI. This obscuring of the lane markings by complex shadows only slightly degrades performance.

TABLE VI
RESULTS FOR THE SPECIAL-CASE SCENARIOS OF TUNNELS AND COMPLEX SHADOWS

	Error Metrics		
	Std. Dev. of Error (cm)	Absolute Mean Error (cm)	Std. Dev. of Error in Rate of Change (cm/s)
Tunnel	22.7438	17.8740	0.51141
Complex Shadows	10.3869	15.4488	0.45682

VI. CONCLUSION

In this paper, we have presented a detailed analysis of the use of lane position in a variety of system objectives, road environments, and sensing systems. We then presented a framework for comparative discussion and evaluation of existing lane-tracking systems. This led to our presentation of the novel VioLET lane-tracking system, a system designed for driver-assistance vehicles operating in a wide range of environments. The VioLET system introduces steerable filters to the lane-detection-and-tracking problem by allowing greater robustness to complex shadowing and lighting changes, while at the same time maintaining a computational simplicity necessary for fast implementations. Using both vehicle-state information as well as visual cues (lane markings and lane texture), we created robust estimates of lane curvature both with and without lookahead visibility. Finally, we provided a detailed analysis of our system with an extensive set of experiments using a unique instrumented-vehicle test bed. This evaluation allowed us to compare performances between different types of road markings at different times of the day, different types of driving situations, and special-case scenarios, which can be critical points in driver-assistance systems.

Along with providing metrics for evaluating system performance, it is also important to note the dependence of various driver-assistance systems to the metrics provided by the underlying sensing algorithms. An example of this is providing the departure rate to a lane-departure-warning system, which can enhance the performance of such systems. Systems have been designed to provide good performance based on a subset of data that is required to accurately predict the exact motion of the vehicle within the lane [38]. With this in mind, we plan on identifying and exploring further the types of metrics useful for various driver-assistance systems. An example of this work can be seen in [1] and [8].

Specific examples of the types of system objectives that this lane-position tracker was designed to be used on are those described in [43]–[45]. These systems are designed to capture the complete vehicle context including vehicle surround, vehicle state, and driver state. By capturing the complete vehicle context, we open the possibility of developing driver-assistance systems focused on the driver and his or her intended actions [8].

ACKNOWLEDGMENT

The authors of this paper would like to thank UC Discovery Grant (Digital Media Innovations program), Nissan Motor Co. Ltd., and their colleagues at the Computer Vision and Robotic Research Laboratory, especially Dr. T. Gandhi and O. Achler.

REFERENCES

[1] J. McCall and M. M. Trivedi, "Visual context capture and analysis for driver attention monitoring," in *Proc. IEEE Conf. Intelligent Transportation Systems*, Washington, DC, Oct. 2004, pp. 332–337.
[2] D. D. Salvucci, "Inferring driver intent: A case study in lane-change detection," in *Proc. Human Factors Ergonomics Society 48th Annu. Meeting*, New Orleans, LA, 2004, pp. 2228–2231.
[3] N. Kuge, T. Yamamura, and O. Shimoyama, *A Driver Behavior Recognition Method Based on a Driver Model Framework*. Warrendale, PA: Soc. Automot. Eng., 1998.
[4] W. Kwon and S. Lee, "Performance evaluation of decision making strategies for an embedded lane departure warning system," *J. Robot. Syst.*, vol. 19, no. 10, pp. 499–509, Sep. 2002.
[5] F. Heimes and H.-H. Nagel, "Towards active machine-vision-based driver assistance for urban areas," *Int. J. Comput. Vis.*, vol. 50, no. 1, pp. 5–34, Oct. 2002.
[6] W. Enkelmann, "Video-based driver assistance—From basic functions to applications," *Int. J. Comput. Vis.*, vol. 45, no. 3, pp. 201–221, Dec. 2001.
[7] The Johns Hopkins University Applied Physics Laboratory, "Survey of on-board technologies applicable to commercial vehicle operations," U.S. Dept. Transportation, Washington, D.C., Tech. Rep. 1998. [Online]. Available: http://cvisn.fmcsa.dot.gov/downdocs/cvisndocs/1_general/onboard_tech_survey.pdf
[8] J. McCall, D. Wipf, M. M. Trivedi, and B. Rao, "Lane change intent analysis using robust operators and sparse Bayesian learning," in *Proc. IEEE Int. Workshop Machine Vision Intelligent Vehicles/IEEE Int. Conf. Computer Vision and Pattern Recognition*, San Diego, CA, Jun. 2005, pp. 59–66.
[9] J. McCall, O. Achler, M. M. Trivedi, P. Fastrez, D. Forster, J. B. Haue, J. Hollan, and E. Boer, "A collaborative approach for human-centered driver assistance systems," in *Proc. 7th IEEE Conf. Intelligent Transportation Systems*, Washington, DC, Oct. 2004, pp. 663–667.
[10] H. Godthelp, P. Milgram, and G. J. Blaauw, "The development of a time-related measure to describe driving strategy," *Hum. Factors*, vol. 26, no. 3, pp. 257–268, 1984.
[11] K. Kluge, "Performance evaluation of vision-based lane sensing: Some preliminary tools, metrics, and results," in *Proc. IEEE Intelligent Transportation Systems Conf.*, Boston, MA, 1997, pp. 723–728.
[12] C. Taylor, J. Košecká, R. Blasi, and J. Malik, "A comparative study of vision-based lateral control strategies for autonomous highway driving," *Int. J. Robot. Res.*, vol. 18, no. 5, pp. 442–453, May 1999.
[13] B. Ma, S. Lakshmanan, and A. O. Hero, "Simultaneous detection of lane and pavement boundaries using model-based multisensor fusion," *IEEE Trans. Intell. Transp. Syst.*, vol. 1, no. 5, pp. 135–147, Sep. 2000.
[14] V. Kastrinaki, M. Zervakis, and K. Kalaitzakis, "A survey of video processing techniques for traffic applications," *Image Vis. Comput.*, vol. 21, no. 4, pp. 359–381, Apr. 2003.
[15] M. Bertozzi, A. Broggi, M. Cellario, A. Fascioli, P. Lombardi, and M. Porta, "Artificial vision in road vehicles," *Proc. IEEE—Special Issue on Technology and Tools for Visual Perception*, vol. 90, no. 7, pp. 1258–1271, Jul. 2002.
[16] E. D. Dickmanns and B. D. Mysliwetz, "Recursive 3-D road and relative ego-state recognition," *IEEE Trans. Pattern Anal. Mach. Intell.*, vol. 14, no. 2, pp. 199–213, Feb. 1992.
[17] Y. Wang, E. Teoh, and D. Shen, "Lane detection and tracking using B-snake," *Image Vis. Comput.*, vol. 22, no. 4, pp. 269–280, Apr. 2004.
[18] J. Goldbeck, B. Huertgen, S. Ernst, and L. Kelch, "Lane following combining vision and DGPS," *Image Vis. Comput.*, vol. 18, no. 5, pp. 425–433, Apr. 2000.
[19] D. Pomerleau, "Neural network vision for robot driving," in *The Handbook of Brain Theory and Neural Networks*, M. Arbib, Ed. Cambridge, MA: MIT Press, 1995.
[20] M. Bertozzi and A. Broggi, "GOLD: A parallel real-time stereo vision system for generic obstacle and lane detection," *IEEE Trans. Image Process.*, vol. 7, no. 1, pp. 62–81, Jan. 1998.
[21] K. Kluge and S. Lakshmanan, "A deformable template approach to lane detection," in *Proc. IEEE Intelligent Vehicles Symp.*, Detroit, MI, 1995, pp. 54–59.
[22] S. Nedevschi, R. Schmidt, T. Graf, R. Danescu, D. Frentiu, T. Marita, F. Oniga, and C. Pocol, "3D lane detection system based on stereovision," in *Proc. IEEE Intelligent Transportation Systems Conf.*, Washington, DC, Oct. 2004, pp. 161–166.

[23] Y. Otsuka, S. Muramatsu, H. Takenaga, Y. Kobayashi, and T. Monj, "Multitype lane markers recognition using local edge direction," in *Proc. IEEE Intelligent Vehicles Symp.*, Versailles, France, Jun. 2002, vol. 2, pp. 604–609.
[24] C. Kreucher and S. Lakshmanan, "LANA: A lane extraction algorithm that uses frequency domain features," *IEEE Trans. Robot. Autom.*, vol. 15, no. 2, pp. 343–350, Apr. 1999.
[25] D. Pomerleau and T. Jochem, "Rapidly adapting machine vision for automated vehicle steering," *IEEE Expert—Special Issue on Intelligent System and Their Applications*, vol. 11, no. 2, pp. 19–27, Apr. 1996.
[26] Q. Li, N. Zheng, and H. Cheng, "Springrobot: A prototype autonomous vehicle and its algorithms for lane detection," *IEEE Trans. Intell. Transp. Syst.*, vol. 5, no. 4, pp. 300–308, Dec. 2004.
[27] J. B. McDonald, "Detecting and tracking road markings using the Hough transform," in *Proc. Irish Machine Vision and Image Processing Conf.*, Maynooth, Ireland, 2001, pp. 1–9.
[28] D.-J. Kang and M.-H. Jung, "Road lane segmentation using dynamic programming for active safety vehicles," *Pattern Recognit. Lett.*, vol. 24, no. 16, pp. 3177–3185, Dec. 2003.
[29] N. Apostoloff and A. Zelinsky, "Robust vision based lane tracking using multiple cues and particle filtering," in *Proc. IEEE Intelligent Vehicles Symp.*, Columbus, OH, Jun. 2003, pp. 558–563.
[30] B. Southall and C. J. Taylor, "Stochastic road shape estimation," in *Proc. Int. Conf. Computer Vision*, Vancouver, BC, Canada, 2001, pp. 205–212.
[31] S. Lee and W. Kwon, "Robust lane keeping from novel sensor fusion," in *Proc. IEEE Int. Conf. Robotics and Automation*, Seoul, Korea, 2001, vol. 4, pp. 3704–3709.
[32] F. Chausse, R. Aufrere, and R. Chapuis, "Recovering the 3D shape of a road by on-board monocular vision," in *Proc. 15th Int. Conf. Pattern Recognition*, Barcelona, Spain, 2000, pp. 325–328.
[33] K. Kluge and C. Thorpe, "The YARF system for vision-based road following," *Math. Comput. Model.*, vol. 22, no. 4–7, pp. 213–233, Aug. 1995.
[34] C. Kreucher, S. Lakshmanan, and K. Kluge, "A driver warning system based on the LOIS lane detection algorithm," in *Proc. IEEE Int. Conf. Intelligent Vehicles*, Stuttgart, Germany, Oct. 1998, pp. 17–22.
[35] R. Risack, N. Mohler, and W. Enkelmann, "A video-based lane keeping assistant," in *Proc. IEEE Intelligent Vehicles Symp.*, Dearborn, MI, Oct. 2000, pp. 506–511.
[36] S. Baluja, "Evolution of an artificial neural network based autonomous land vehicle controller," *IEEE Trans. Syst., Man, Cybern. B, Cybern.*, vol. 26, no. 3, pp. 450–463, Jun. 1996.
[37] J. W. Lee, "A machine vision system for lane-departure detection," *Comput. Vis. Image Underst.*, vol. 86, no. 1, pp. 52–78, Apr. 2002.
[38] J. W. Lee, C.-D. Kee, and U. K. Yi, "A new approach for lane departure identification," in *Proc. IEEE Intelligent Vehicles Symp.*, Columbus, OH, 2003, pp. 100–105.
[39] W. T. Freeman and E. H. Adelson, "The design and use of steerable filters," *IEEE Trans. Pattern Anal. Mach. Intell.*, vol. 13, no. 9, pp. 891–906, Sep. 1991.
[40] S. Szabo, K. Murphy, and M. Juberts, "The AUTONAV/DOT project: Baseline measurement system for evaluation of roadway departure warning systems," National Institute of Standards and Technology, Gaithersburg, MD, NISTIR 6300, 1999.
[41] J. McCall, O. Achler, and M. M. Trivedi, "Design of an instrumented vehicle testbed for developing human centered driver support system," in *Proc. IEEE Intelligent Vehicles Symp.*, Parma, Italy, Jun. 2004, pp. 483–488.
[42] J.-Y. Bouguet, *Camera Calibration Toolbox for Matlab*. [Online]. Available: http://www.vision.caltech.edu/bouguetj/calib_doc/
[43] K. Huang, M. M. Trivedi, and T. Gandhi, "Driver's view and vehicle surround estimation using omnidirectional video stream," in *Proc. IEEE Intelligent Vehicles Symp.*, Columbus, OH, Sep. 2003, pp. 444–449.
[44] T. Gandhi and M. M. Trivedi, "Parametric ego-motion estimation for vehicle surround analysis using omni-directional camera," *Mach. Vis. Appl.*, vol. 16, no. 2, pp. 85–89, Feb. 2005.
[45] M. M. Trivedi, S. Y. Cheng, E. M. C. Childers, and S. J. Krotosky, "Occupant posture analysis with stereo and thermal infrared video: Algorithms and experimental evaluation," *IEEE Trans. Veh. Technol.*, vol. 53, no. 6, pp. 1698–1712, Nov. 2004.

Joel C. McCall received the B.S. degree in electrical engineering and computer science from the University of California, Berkeley (UCB), in 1999. He received the M.S. degree in electrical and computer engineering from the University of California, San Diego (UCSD), in 2003. He is currently working toward the Ph.D. degree in electrical and computer engineering, specializing in intelligent systems, robotics, and control at UCSD.

He is currently a Graduate Student Researcher in the Laboratory for Intelligent and Safe Automobiles (LISA) within the Computer Vision and Robotics Research Laboratory at UCSD. His research focuses on human-centered driver-assistance and safety systems.

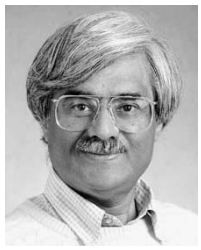

Mohan M. Trivedi received the B.E. degree (with honors) from the Birla Institute for Technology and Science (BITS), Birla, India, in 1974 and the Ph.D. degree from the Utah State University, Logan, in 1979.

He is a Professor of electrical and computer engineering and the founding Director of the Computer Vision and Robotics Research Laboratory at the University of California, San Diego (UCSD). In partnership with several automobile companies, he established the Laboratory for Intelligent and Safe Automobiles ("LISA") at UCSD to pursue a multidisciplinary research agenda. He has published nearly 300 technical articles and has edited over a dozen volumes including books, special issues, video presentations, and conference proceedings. His research interests include intelligent systems, computer vision, intelligent ("smart") environments, intelligent vehicles and transportation systems, and human-machine interfaces areas.

Dr. Trivedi was the Editor-in-Chief of the *Machine Vision and Applications Journal*. He served as the Chairman of the Robotics Technical Committee of the Computer Society of the IEEE and on the Administrative Committee (ADCOM) of the IEEE SMC Society. He serves on the Executive Committee of the California Institute for Telecommunication and Information Technologies [Cal-IT2] as the leader of the Intelligent Transportation and Telematics Layer at UCSD. He regularly serves as a Consultant to industry and government agencies in the USA and abroad. He received the Distinguished Alumnus Award from the Utah State University, the Pioneer Award (Technical Activities), and the Meritorious Service Award from the IEEE Computer Society.